Crystal Structure of κ-Bungarotoxin at 2.3-Å Resolution[†,‡]

John C. Dewan,[§] Gregory A. Grant,[∥] and James C. Sacchettini*[,§]

Department of Biochemistry, Albert Einstein College of Medicine, Bronx, New York 10461, and Departments of Medicine and of Molecular Biology and Pharmacology, Washington University School of Medicine, St. Louis, Missouri 63110

Received July 15, 1994; Revised Manuscript Received August 11, 1994[⊗]

ABSTRACT: κ-Neurotoxins display a very low affinity for neuromuscular receptors, but bind tightly to, and inhibit, nicotinic acetylcholine receptors in neuronal tissue such as the chick ciliary ganglia. In contrast, α-neurotoxins bind with high affinity and inhibit nicotinic acetylcholine receptors at the neuromuscular junction. The origin of this difference in specificity has been a long-studied question in the field. Here we report the first crystal structure of a κ-neurotoxin, κ-bungarotoxin. Unlike the NMR structure previously reported [Sutcliffe, M. J., Dobson, C. M., & Oswald, R. E. (1992) *Biochemistry 31*, 2962–2970], the present crystal structure more accurately defines the polypeptide fold and the nature of the interaction between subunits in the active dimer, which is a unique feature of the κ-neurotoxins. The structure has been refined to $R = 19.6\%$ with X-ray diffraction data extending to a resolution of 2.3 Å. There are two independent protein molecules (66 amino acid residues each) in the asymmetric unit that are arranged as a dimer with the two subunits related by a rotation of 178.6°. Each subunit consists of three main-chain loops. Three of the five β-strands of each subunit form an antiparallel β-sheet which becomes an extended six-stranded antiparallel β-sheet, by virtue of the approximate 2-fold symmetry of the dimer. The interactions at the dimer interface consist of six main-chain–main-chain hydrogen bonds, as well as three other hydrogen-bonding interactions involving side chains. Residues Phe 49 and Leu 57 are found in all four κ-bungarotoxins that have been sequenced, but occur in no α-neurotoxins, and they form van der Waals interactions across the dimer interface. The two subunits of the dimer are not identical, with the major difference between them occurring at the tip of the central loop (Cys 27–Pro 36). Residue Arg 34, which is essential for the activity of both α- and κ-neurotoxins, occurs at the tip of the central loop in each subunit, with guanidinium groups that are ~44 Å apart.

The venom of the hydrophid and elapid families of snakes contains a broad class of structurally related toxins that affect nerve transmission (Rodriguez-Ithurralde et al., 1983; Endo & Tamiya, 1991; Rees & Bilwes, 1993). Among these toxins there is a high degree of identity between their amino acid sequences, including 4–5 conserved disulfide bridges. Moreover, all of the structures determined so far show similar polypeptide folds. The toxins are distinguished by their fundamentally different modes of action and include postsynaptic neurotoxins, cytotoxins, and fasciculins. The postsynaptic neurotoxins are high-affinity acetylcholine antagonists that inhibit signal transmission across the synapse by binding to the α-subunits of the postsynaptic nicotinic receptor. The site of action of the cytotoxins is unclear, but their effect appears to be persistent membrane depolarization, while the fasciculins are acetylcholinesterase inhibitors.

The muscle nicotinic acetylcholine receptor is the best characterized postsynaptic receptor, largely due to the utilization of the curaremimetic α-neurotoxin group of small snake venom-derived polypeptides (Endo & Tamiya, 1991). More recently, the discovery of the κ-neurotoxins (Chiappinelli, 1983) has made it possible to study, in a similar manner, nicotinic acetylcholine receptors in various neuronal tissues (Galzi et al., 1991).

κ-Bungarotoxin is a 66 residue polypeptide present (~0.1–0.2%, w/w) in the venom of the Taiwanese banded krait, *Bungarus multicinctus*, which displays distinct sequence homology with the α-neurotoxins (Grant & Chiappinelli, 1985). κ-Bungarotoxin is a member of a small group of related proteins that possess the ability to selectively block nicotinic transmission by interaction with neuronal nicotinic acetylcholine receptors, such as those found in the ciliary and sympathetic ganglia of the chick (Chiappinelli & Zigmond, 1978; Chiappinelli, 1983; Chiappinelli & Dryer, 1984; Fiordalisi et al., 1994a). This is in sharp contrast to the larger group of α-neurotoxins that block the function of nicotinic acetylcholine receptors in vertebrate skeletal muscle and electric fish electric organ. The α-neurotoxins have no effect on the neuronal receptors that are the targets of the κ-neurotoxins. Thus, the κ-neurotoxins affect receptors of neuronal origin, while the α-neurotoxins block nerve transmission at the muscle end plate. Moreover, while α-neurotoxins bind to components in some neuronal tissues, they do not appear to affect nerve transmission in these tissues. One further distinction is that the κ-neurotoxins are homodimers in solution, as opposed to the α-neurotoxins, which all appear to be monomeric.

The three-dimensional structures of several α-neurotoxins have been determined by X-ray crystallography. These are erabutoxin *a* [Corfield et al., 1989; Protein Data Bank (PDB) (Bernstein et al., 1977) entry code 5EBX], erabutoxin *b* (Low et al., 1976; Tsernoglou & Petsko, 1976; Bourne et al., 1985; Low & Corfield, 1986, 1987; Smith et al., 1988; PDB entry codes 3EBX and 6EBX), α-bungarotoxin (Love & Stroud, 1986; PDB entry code 2ABX), and α-cobratoxin (Betzel et al., 1991; PDB entry code 2CTX). The crystal structures of the related cardiotoxin V_4^{II} (Rees et al., 1990; PDB entry code 1CDT) and the anti-acetylcholinesterase toxin, fasciculin 1 (le Du et al., 1992; PDB entry code 1FAS) have also been determined. All of these structures are very similar, consisting

[†] Supported by NIH Grants GM 50624 (formerly NS 28447) to G.A.G. and GM 45859 and AI 33696 to J.C.S.

[‡] Coordinates and observed structure factors for the κ-bungarotoxin crystal structure have been deposited with the Brookhaven Protein Data Bank as entry 1KBA.

[§] Albert Einstein College of Medicine.

[∥] Washington University School of Medicine.

[⊗] Abstract published in *Advance ACS Abstracts,* October 1, 1994.

0006-2960/94/0433-13147$04.50/0

Table 1: Data Collection Statistics for Native and Derivative Data Sets[a]

	resolution (Å)	no. unique reflections	completeness of data (%)	R_{merge}[b]	R_{iso}[c]	$I/\sigma(I)$	redundancy[d]	soak concn (mM)	soak time (days)
native	2.3	6602	99	0.068		8.6	3.2		
$K_2[PtCl_4]$	3.0	3018	99	0.103	0.119	9.9	6.7	1	1
$UO_2(NO_3)_2 \cdot 6H_2O$ (no. 1)	3.0	3026	99	0.119	0.183	7.4	3.2	4	1
$UO_2(NO_3)_2 \cdot 6H_2O$ (no. 2)	3.0	2606	85	0.212	0.344	4.2	4.0	10	1
$K_2[Pt(NO_2)_4]$	3.0	3038	99	0.098	0.164	9.4	3.2	2	1
$Hg(CH_3CO_2)_2$	3.6	1627	92	0.246	0.162	7.1	4.6	4	2

[a] No sigma cutoff was applied to any of the data referred to in this table. [b] $R_{merge} = \sum\sum_i |I_i - \langle I \rangle| / \sum \langle I \rangle$, where I_i is the scale factor corrected intensity for a reflection and $\langle I \rangle$ is the mean intensity for that reflection. [c] $R_{iso} = \sum |F_{PH}^2 - F_P^2| / \sum (F_{PH}^2 + F_P^2)$, where F_{PH} and F_P are the derivative and native structure factor amplitudes, respectively. [d] Total reflections collected/unique reflections.

Table 2: Heavy-Atom Parameters and Phasing Statistics

derivative	site	x[a]	y	z	B[b]	occupancy	R_C[c]	$\langle F_H \rangle / E$[d]	FOM[e]
$K_2[PtCl_4]$	PTCL1	0.557	0.883	0.845	28.42	1.14	0.639	1.16	0.30
	PTCL2	0.321	0.869	0.108	40.12	0.90			
$UO_2(NO_3)_2 \cdot 6H_2O$ (no. 1)	U11	0.601	0.870	0.000[f]	31.22	1.47	0.520	1.83	0.37
	U12	0.302	0.974	0.471	45.49	0.91			
	U13	0.558	0.783	0.931	47.37	1.37			
	U14	0.312	0.731	0.931	48.44	0.91			
$UO_2(NO_3)_2 \cdot 6H_2O$ (no. 2)	U21	0.355	0.937	0.826	27.59	1.24	0.578	2.01	0.32
	U22	0.386	0.969	0.529	25.73	1.12			
	U23	0.474	0.786	0.427	75.45	1.02			
$K_2[Pt(NO_2)_4]$	PTNO1	0.385	0.704	0.632	8.04	1.12	0.615	1.22	0.31
	PTNO2	0.451	0.865	0.326	33.48	1.28			
	PTNO3	0.465	0.803	0.242	45.53	1.28			
$Hg(CH_3CO_2)_2$	HG1	0.320	0.695	0.472	54.26	1.25	0.593	1.44	0.34

[a] Fractional atomic coordinates. [b] Isotropic temperature factor (Å^2). [c] Cullis R-factor = $\sum ||F_{PH} \pm F_P| - |F_H|| / \sum |F_{PH} \pm F_P|$ for centric reflections, where F_{PH}, F_P, and F_H are the derivative, native, and calculated heavy-atom structure factor amplitudes. [d] Phasing power, where $\langle F_H \rangle$ is the mean of the calculated heavy-atom structure factor amplitude and E is the residual lack-of-closure error. [e] Mean figure of merit for both centric and acentric reflections. [f] Arbitrary value to fix space group origin.

of what are traditionally described as three main-chain loops (Low, 1979) containing four or five disulfide bridges. In all structures, the two strands of the central loop and the second β-strand of the third loop constitute a three-stranded antiparallel β-pleated sheet.

Until now, no crystal structure of a κ-neurotoxin has been available, although a solution structure of κ-bungarotoxin from nuclear magnetic resonance (NMR) data has been reported (Oswald et al., 1991; Sutcliffe et al., 1992; PDB entry code 1NBT). That work indicated that κ-bungarotoxin has a conformation similar to those of the α-neurotoxins, in that a triple-stranded β-sheet is the major component of secondary structure. In addition, two residues contributing main-chain–main-chain hydrogen-bonding interactions to the dimer interface of κ-bungarotoxin in solution were identified. No such interface was indicated in the NMR studies of the α-neurotoxins (Hider et al., 1982; Inagaki et al., 1985; Basus et al., 1988; Labhardt et al., 1988), nor was one expected. The NMR structure of κ-bungarotoxin contained several areas, however, where uncertainty existed. These include uncertainty at the dimer interface and concerning the location, relative to the rest of each subunit, of the loop consisting of Arg 1–Ile 20 as well as the C-terminal tail consisting of residues Thr 60–His 66. The relatively small number of long range NOEs in these areas has prevented the emergence of a definitive structure from these studies, and 12 individual structures were reported that differ significantly in these regions. Here we report the first X-ray structure of a κ-neurotoxin, κ-bungarotoxin, refined to a conventional R-factor of 19.6% with X-ray diffraction data to 2.3-Å resolution. The structure is well defined in all respects and significantly reduces the uncertainty in the NMR structure.

EXPERIMENTAL PROCEDURES

Crystallization. Sacchettini et al. (1992) previously described the crystallization of κ-bungarotoxin. The protein was purchased from Biotoxins, Inc. (St. Cloud, FL) and further purified by reverse-phase HPLC (Fiordalisi, 1994). Crystals of the 66 residue protein are hexagonal, space group $P6$, with $a = b = 80.2$ Å, $c = 39.6$ Å, $\alpha = \beta = 90°$, and $\gamma = 120°$. There are two protein molecules in the asymmetric unit ($Z = 12$), and the crystals contain 58% solvent. Crystal dimensions were typically 0.25 mm × 0.25 mm × 0.15 mm.

Data Collection and Processing. All data sets were collected at room temperature using Cu Kα radiation ($\lambda = 1.5418$ Å), with a Siemens multiwire area detector coupled to a Rigaku RU-200 rotating anode generator. One crystal was used for each data set, and data reduction was carried out with the XENGEN package of programs (Siemens Analytical X-ray Instruments, Madison, WI). Details and statistics for the X-ray diffraction data sets are described in Table 1.

Structure Determination. Initial attempts to solve the structure using the molecular replacement technique were unsuccessful. Search models included the crystal structures of the α-neurotoxins, as well as the 12 κ-bungarotoxin NMR structures (Sutcliffe et al., 1992; PDB entry code 1NBT).

The κ-bungarotoxin crystal structure was solved by the multiple isomorphous replacement (MIR) technique (Blundell & Johnson, 1976) using the heavy-atom derivatives listed in Table 2. The PHASES package of programs (Furey & Swaminathan, 1990) was employed for all calculations unless otherwise noted. Heavy-atom positions for the $K_2[PtCl_4]$ derivative were determined from an isomorphous difference Patterson map. Positions for the other derivatives were located on difference Fourier maps and confirmed with difference Patterson maps. The anomalous scattering contributions of

the $K_2[PtCl_4]$ and $UO_2(NO_3)_2 \cdot 6H_2O$ (no. 1) derivatives were both used to assign the correct hand to the structure (Blundell & Johnson, 1976), although the anomalous data were not used in subsequent protein phasing calculations as their inclusion did not contribute to the quality of the resulting electron density map. Heavy-atom refinement (Table 2) followed by calculation of protein phases yielded an overall mean figure of merit of 0.61, which improved to 0.83 upon solvent flattening (Wang, 1985). The quality of the electron density map, calculated at 3-Å resolution, was sufficient to identify a six-stranded β-sheet representing the κ-bungarotoxin dimer, and the structure was built into this electron density using the model-building program TOM, a derivative of FRODO (Jones, 1985). The electron density was not subjected to noncrystallographic symmetry averaging, and noncrystallographic symmetry constraints were not applied at any stage of the refinement.

Metal Binding Sites. The only potential protein ligand available for covalent attachment of metal complexes in κ-bungarotoxin is the side chain of His 66, which is located at the C-terminus of each subunit. The $K_2[Pt(NO_2)_4]$ sites (Table 2) are all close to either His 66 or His 66′, and the $Hg(CH_3CO_2)_2$ site is close to His 66′, suggesting that binding has occurred between the side chain of this residue and the metal atoms of both compounds. Somewhat surprisingly, the two $K_2[PtCl_4]$ sites occur close to the Cys 27–Cys 31 disulfide bridge at the tip of loop II (see below) in each subunit, suggesting that both disulfide bridges have opened and the sulfur atoms are binding in a covalent fashion to Pt(II) in each case. The two $UO_2(NO_3)_2 \cdot 6H_2O$ derivatives do not share common sites (Table 2), probably due to the different soaking concentrations used in each case, but all lie close to Asp or Glu residues, while one site occurs at the carboxy terminus of subunit 2.

Structure Refinement. Rigid body refinement with X-PLOR (Brünger, 1992), treating the two subunits of the dimer as separate entities, gave an *R*-factor of 50.5% for data in the resolution range 13–3 Å. Refinement of the structure by simulated annealing, using the slow-cooling protocol of Brünger et al. (1990), yielded $R = 31.3\%$ for the data between 6- and 2.5-Å resolution. Several rounds of simulated annealing with X-PLOR and manual model building with TOM were subsequently performed to improve the model. Electron density maps examined during this process were calculated with coefficients $(2|F_o| - |F_c|, \phi_c)$ and $(|F_o| - |F_c|, \phi_c)$, as were $2|F_o| - |F_c|$ electron density maps that employed a combination of MIR and model-based phases (Furey & Swaminathan, 1990). The final stage of refinement was continued with TNT (Tronrud et al., 1988), employing the standard geometry of Engh and Huber (1991) as implemented by Priestle (1993). This included the refinement of restrained individual isotropic *B*-factors for each atom. Before the inclusion of water molecules, the *R*-factor was 22.0% for the 5354 reflections (80% complete) in the resolution range 13–2.3 Å. Data with $I > \sigma(I)$ were used in all refinements. The final model ($R = 19.6\%$) consists of 1002 non-hydrogen protein atoms and 56 water molecules with root-mean-square (rms) deviations of bond lengths and angles from ideality of 0.022 Å and 2.79°, respectively. For the 4616 reflections (70% complete) with $I > 2\sigma(I)$, the *R*-factor was 17.9%. All residues are included in the model, and all lie within allowed regions of the Ramachandran plot (Laskowski et al., 1993).

Crystal Packing. The κ-bungarotoxin dimers all pack such that their long axis, which corresponds to the axis of loop II (see below), is parallel to the *c*-axis of the unit cell, and they all span the cell from $z \sim 0$ to $z \sim 1$, giving a value of ~40 Å to the dimer in this direction since the *c* unit cell dimension is 39.6 Å. Large solvent channels, with 6-fold symmetry and a diameter of ~35 Å, are centered at each corner of the unit cell, while smaller solvent channels, with 3-fold symmetry and a diameter of ~15 Å, are centered at $(x = 1/3, y = 2/3)$ and $(x = 2/3, y = 1/3)$. Both types of channel are infinite and run parallel to the *c*-axis. The majority of the heavy-atom derivatives bind within these channels, and both His 66 and His 66′ are solvent accessible since they face into the channels with 3-fold symmetry.

The phenyl ring of Phe 30′ (subunit 2) interacts with Phe 30′ of the dimer located at $(-x, -y, z)$ in what is presumably 50% disorder, with one phenyl ring directed at the π-electron cloud of the other and *vice versa*, thus forming aromatic–aromatic interactions with one another (Burley & Petsko, 1985).

RESULTS AND DISCUSSION

Crystals of κ-bungarotoxin contain two molecules (66 amino acid residues each) per asymmetric unit that are arranged as a dimer having approximate 2-fold noncrystallographic symmetry (Figures 1 and 2). The two molecules that make up the dimer are referred to as subunits 1 and 2, with the various features of subunit 2 (e.g., residues and β-strands) being designated by a prime (′) in the text that follows.

Description of the Structure. Each subunit of the dimer is composed of three main-chain loops that are approximately defined by residues Arg 1–Cys 14 (loop I), Cys 21–Cys 42 (loop II), and Cys 46–Cys 58 (loop III), along with a C-terminal tail defined by residues Cys 59–His 66 (Figure 3). Loops I and III are shorter than the longer central loop II. In addition, each subunit contains five highly conserved disulfide bridges: Cys 3–Cys 21, Cys 14–Cys 42, Cys 27–Cys 31, Cys 46–Cys 58, and Cys 59–Cys 64 (Figure 2).

Superposition of the two subunits of the κ-bungarotoxin homodimer reveals that they are not identical. The rms difference between the CA atoms is 1.2 Å and that between all atoms is 1.7 Å. The major difference between the subunits occurs in the position of residues 27–36 at the tip of loop II. If these residues are excluded from the superposition calculation, the rms values drop to 0.7 Å for CA atoms and 1.2 Å for all atoms. A second region of the protein where the subunits deviate is the turn comprising residues 15–18. If these residues are also excluded from the superposition, the rms difference becomes 0.5 Å for CA atoms while remaining 1.2 Å for all atoms.

The two β-strands of loop II (β-strands C and D) and the C-terminal β-strand of loop III (β-strand E) form a central three-stranded antiparallel β-sheet (Table 3 and Figures 1 and 2) that has an overall right-handed twist (Salemme & Weatherford, 1981). There are slight differences between the subunits in the composition of this β-sheet. Overall, however, the structure contains eight main-chain–main-chain hydrogen bonds between strands C and D (loop II) and six such hydrogen bonds between strand C (loop II) and strand E (loop III), with 3.5 Å being taken as the upper limit for a hydrogen bond (Figure 3). The latter set of interactions serves to link loops II and III. In subunit 1 there is a hydrogen bond between the amide proton of Ile 20 and the carbonyl group of Val 43, but this interaction is slightly longer in subunit 2 (Ile 20—N···Val 43—O = 3.4 Å, Ile 20′—N···Val 43′—O = 3.8 Å). Conversely, Asp 19 and Val 43 form a similar hydrogen bond in subunit 2 that is longer in subunit 1 (Asp 19—N···Val 43—O = 3.6 Å, Asp 19′—N···Val 43′—O = 3.3 Å). Also,

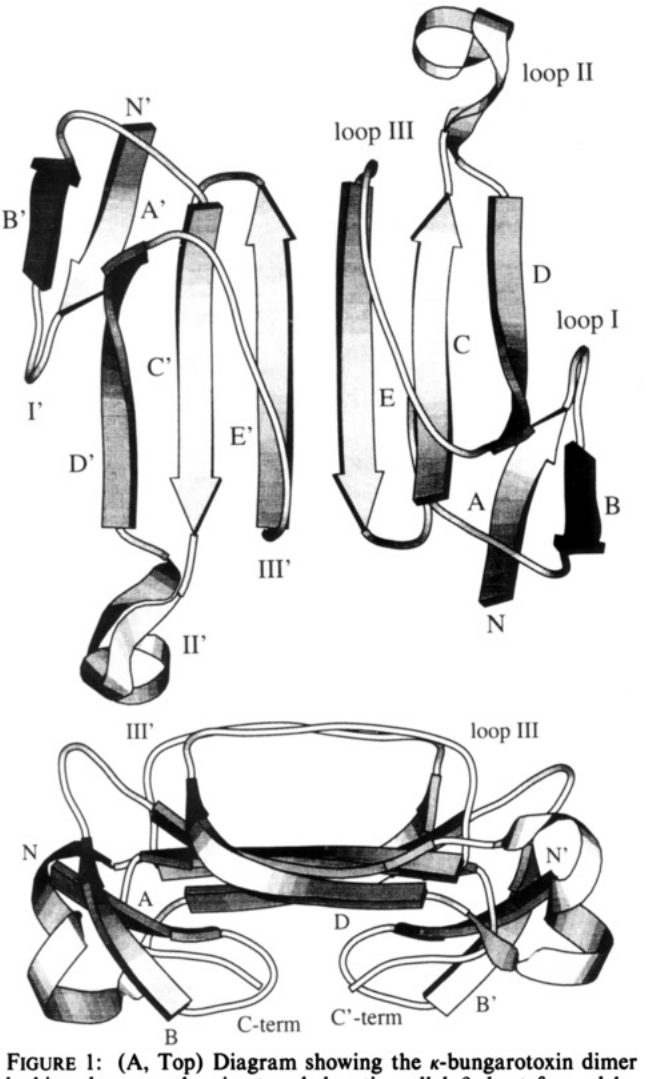

FIGURE 1: (A, Top) Diagram showing the κ-bungarotoxin dimer looking down on the six-stranded antiparallel β-sheet formed by β-strands D-C-E-E′-C′-D′. The N-termini, β-strands, and loops I–III are labeled. The C-termini are obscured by strand C in both subunits. Subunit 1 is on the right, and the labels of subunit 2 are primed. The noncrystallographic 2-fold axis relating the two subunits lies perpendicular to the page and mid-way between β-strands E and E′. (B, Bottom) Diagram of the dimer showing a side view of the six-stranded β-sheet. Loops III and III′ stand perpendicular to the sheet. Subunit 1 is in front, and β-strand D is the first strand of the β-sheet. The N- and C-termini are labeled, as are some of the β-strands along with loops III and III′. Diagrams were produced with MOLSCRIPT (Kraulis, 1991).

a hydrogen bond exists between the carbonyl of Ala 25 and the amide group of Ser 55 in subunit 2 that is longer in subunit 1 (Ala 25—O···Ser 55—N = 3.6 Å, Ala 25′—O···Ser 55′—N = 3.2 Å) (Figure 3). Because of the slightly different orientation of the tip of loop II in each subunit, subunit 1 possesses a hydrogen bond between the amide group of Cys 27 (loop II) and the carbonyl of Asn 52 (loop III) that is not present in subunit 2 (Cys 27—O···Asn 52—N = 3.0 Å, Cys 27′—O···Asn 52′—N = 8.4 Å).

Of the five disulfide bridges, Cys 27–Cys 31 is internal to loop II at its tip, Cys 46–Cys 58 is internal to loop III, and Cys 59–Cys 64 connects the C-terminal tail to strand E of loop III (Figure 2). Only Cys 3–Cys 21 and Cys 14–Cys 42 link different loops together (loops I and II). Hydrogen bonds, rather than disulfide bridges, link loops II and III. The CA···CA distances of the 10 independent disulfide bridges of the dimer (Table 4) range in length from 4.8 to 6.2 Å (av 5.6 Å), which is in accord with the usual range for such interactions (Richardson, 1981). As with erabutoxin, α-cobratoxin, cardiotoxin V_4^{II}, and fasciculin 1, the two bridges that link loops I and II are left-handed (χ_3 near −90°) while the two involved with loop III and the C-terminal tail are right-handed (χ_3 near +90°). The fifth bridge, at the tip of loop II in κ-bungarotoxin and α-cobratoxin, is also left-handed, and the other torsion angles of this bridge in these two structures are all similar. As noted by Rees et al. (1990), the bridge in the C-terminal tail of cardiotoxin V_4^{II} is unusual in that it is symmetric and the mirror image of the most commonly encountered conformation. This is also the case in the present structure and for the structures of erabutoxin, α-cobratoxin, and fasciculin 1.

The polypeptide chain connecting β-strands C and D at the tip of loop II (residues 27–36) in both subunits is folded into two pseudohelical turns that include two type I β-turns involving main-chain–main-chain hydrogen bonds between Asp 28 and Cys 31 and between Phe 30 and Ile 33 (Figure 3). In addition, there are two α-helical i to $i + 4$ main-chain–main-chain hydrogen bonds between Phe 30 and Arg 34 and between Cys 31 and Gly 35 in subunit 1 and one such interaction between Phe 30′ and Arg 34′ in subunit 2. The second interaction in subunit 2 is slightly longer (Cys 31′—O···Gly 35′—N = 3.8 Å). The fifth disulfide bridge of each subunit, Cys 27–Cys 31, also forms part of this structural feature.

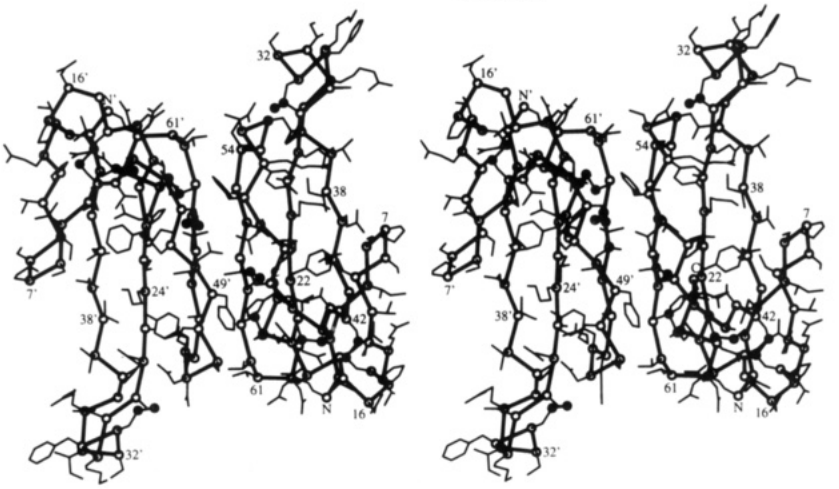

FIGURE 2: Stereodiagram of the κ-bungarotoxin dimer. The CA trace is depicted, and certain of the CA atoms are labeled. Subunit 2 is on the left and its CA atoms are primed. All side chains are shown, as are the disulfide bridges. Open circles are CA atoms, and filled circles are S atoms. The diagram was produced with MOLSCRIPT (Kraulis, 1991).

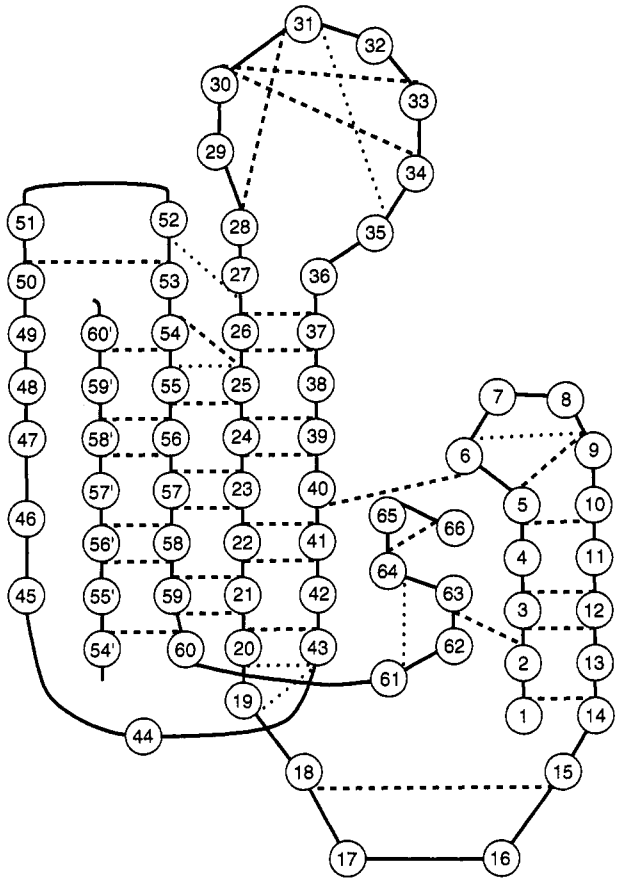

FIGURE 3: Schematic diagram of all main-chain–main-chain hydrogen bonds <3.5 Å. Dashed lines indicate a hydrogen bond present in both subunits, while a dotted line indicates a hydrogen bond present in only one subunit. Proceeding from the N- to the C-terminus (Arg 1 to His 66), the bottom of each circle represents the main-chain amide group of a particular residue, while the top of each circle represents its main-chain carbonyl group. Residues 54–60 (β-strand E′ of subunit 2) are indicated by a prime. The noncrystallographic 2-fold axis relating the two subunits lies perpendicular to the page and mid-way between residues 57 and 57′.

Table 3: Definition of β-Strands[a]

β-strand	residue range
A	1–5
B	10–14
C	20–26
D	37–43
E	54–60

[a] Applies to both subunits of the dimer.

Residues Gln 26 and Gln 26′, which replace what is an invariant Trp residue in the α-neurotoxins, form side-chain–side-chain hydrogen bonds with Arg 50 and Asn 52′, respectively (Table 5). Gln 26 lies on the same side of each κ-bungarotoxin subunit as the invariant Trp residue in all known α-neurotoxin X-ray structures, with the exception of α-bungarotoxin where it is on the other side.

The Dimer Interface. Analytical ultracentrifugation analysis provides evidence that κ-bungarotoxin exists as a dimer in solution (Chiappinelli & Lee, 1985; Oswald et al., 1991; Fiordalisi & Grant, 1994). Analysis of the crystal packing of the κ-bungarotoxin dimer in the *P*6 space group reveals that the two subunits are related by a near 2-fold symmetry axis with a rotation of 178.6° between them.

There are six main-chain–main-chain hydrogen bonds across the dimer interface in the κ-bungarotoxin structure between strand E of subunit 1 and strand E′ of subunit 2 (Figure 3). The amide protons and carbonyl oxygens of residues Leu 56 and Cys 58 hydrogen bond with their counterparts from Cys 58′ and Leu 56′. The fifth and sixth hydrogen bonds are between the carbonyl of Arg 54 (and Arg 54′) and the amide of Thr 60′ (and Thr 60). These interactions serve to extend the three-stranded antiparallel β-sheet of one subunit to a six-stranded antiparallel β-sheet composed of β-strands D-C-E-E′-C′-D′ (Figures 1 and 2). This extended β-sheet also has an overall right-handed twist.

In addition to the main-chain–main-chain interactions discussed here, there are two additional hydrogen-bonding interactions at the dimer interface between the side chains of Gln 48 and Gln 48′. There is also a hydrogen bond between

Table 4: Disulfide Bridges[a]

Cys–Cys	χ_1	χ_2	χ_3	χ_2'	χ_1'	CA···CA
3–21	−65	−64	−86	−47	−59	5.4
	−83	−52	−97	−40	−65	5.3
14–42	−53	−41	−83	−101	−62	5.7
	−61	−47	−95	−83	−72	5.6
27–31	−71	−67	−51	158	−153	4.8
	−88	−61	−48	188	−156	5.0
46–58	−177	73	94	156	−86	6.1
	−186	72	98	174	−97	5.9
59–64	57	93	84	91	58	5.9
	53	101	87	93	60	6.2

[a] The five torsion angles (deg) are listed for each bridge, as is the distance (angstroms) between the two CA atoms. χ_1 and χ_1' are the torsion angles around the two CA–CB bonds, χ_2 and χ_2' are those around CB–SG, and χ_3 is that around SG–SG. The two lines for each entry contain the values for the two independently refined subunits, with those for subunit 1 on top.

Table 5: Main-Chain–Side-Chain and Side-Chain–Side-Chain Hydrogen Bonds[a]

	subunit 1	subunit 2
Intrasubunit Interactions[b]		
Arg 1–NE···Asp 19–O	2.6	2.3
Ser 8–OG···Ile 5–O	3.5	
Gln 18–NE2···Cys 42–O	2.6	
Lys 24–NZ···Glu 39–OE1	3.3	3.1
Gln 26–OE1···Arg 50–NH2	3.2	
Gln 26–NE2···Arg 50–NH2	3.3	
Gln 26–OE1···Asn 52–ND2		3.0
Asp 28–OD1···Cys 31–N	3.1	3.5
Asp 28–OD2···Arg 34–NH1	2.9	2.5
Asp 28–OD2···Arg 34–NH2		3.3
Gln 40–NE2···Ser 9–OG	3.0	
Gln 40–OE1···Ser 9–OG	3.0	3.0
Gln 40–N···Ser 6–OG	3.2	
Gln 40–NE2···Ser 6–O	2.6	
Gln 40–NE2···Asn 65–O		2.8
Arg 50–NE···Tyr 53–OH	3.5	
Asp 62–OD1···Arg 1–NH1	2.5	2.8
Asp 62–OD1···Thr 2–N	3.3	
Asn 63–ND2···Thr 2–O	3.1	2.3
Asn 63–ND2···Thr 2–OG1	3.5	
Asn 65–OD1···Leu 4–N	3.1	2.7
Asn 65–ND2···Leu 4–O	3.2	2.8
Asn 65–ND2···Phe 22–O	3.0	3.0
His 66–ND1···Asn 63–O	3.4	
His 66–ND1···Cys 64–O	3.3	2.4
Intersubunit Interactions[c]		
Gln 48–OE1···Gln 48′–NE2	2.6	
Gln 48–NE2···Gln 48′–OE1	2.9	
Thr 60–OG1···Tyr 53′–O	3.2	

[a] Interactions <3.5 Å are listed. [b] Note that primes are not employed here to denote subunit 2. A blank entry under a heading implies that interaction occurs only within the other subunit. [c] Interactions across the dimer interface are indicated by a prime.

Thr 60 and Tyr 53′ that is longer in the other direction (Tyr 53–O···Thr 60′–OG1 = 3.6 Å) (Table 5, Figure 2). The interaction between Gln 48 and Gln 48′ is the only hydrogen bond between the non-β-sheet strand of loops III and III′. Gln 48 may not be crucial to dimer formation, however, since only two of the four κ-bungarotoxins for which a sequence is available possess Gln at this position (Fiordalisi et al., 1994a). This Gln residue is Glu in the other two sequences, which would not be expected to form a hydrogen bond with its symmetry mate, across the dimer interface, at physiological pH.

Further dimer interactions in κ-bungarotoxin are provided by van der Waals interactions between the aromatic ring of Phe 49 and the side chains of Ile 20′, Thr 60′, and the Cys 46′–Cys 58′ disulfide bridge. These groups are all within ~4 Å of Phe 49 (Phe 49—CZ···Ile 20′—CD1 = 3.9 Å, Phe 49—CZ···Thr 60′—CG2 = 4.1 Å, Phe 49—CG···Cys 46′—CB = 3.4 Å, Phe 49—CE1···Cys 58′—CB = 3.8 Å). Because of the approximate 2-fold symmetry of the dimer, similar interactions also occur between Phe 49′ and the equivalent residues of subunit 1. An additional set of van der Waals contacts across the dimer interface involves the side-chain atoms of Leu 57 and Leu 57′, which are ~4 Å from one another (Leu 57—CD1···Leu 57′—CD1 = 4.3 Å). Both residues Phe 49 and Leu 57 are found in all four κ-bungarotoxins for which sequences are available (Fiordalisi et al., 1994a) but are not found in the α-neurotoxins, and their van der Waals interactions across the dimer interface probably contribute to the observed solution dimer. Of the 958 Å^2 of each subunit buried by dimer formation, 34% is formed by hydrophobic residues, 51% by polar residues, and 10% by charged residues. Although the κ-neurotoxins are the only group of the structurally related toxins to dimerize in solution, many of the α-neurotoxins, whose crystal structures have been determined, pack together in the crystal with an orientation and interface similar to those of κ-bungarotoxin. The significance of this is unclear.

Comparison of the κ-Bungarotoxin X-ray and NMR Structures. Of the 12 structures generated in the NMR analysis (Sutcliffe et al., 1992), structures 4 and 12 most closely approximate the conformation found in the crystal structure, while structures 8 and 9 display the largest deviations. When subunits of the X-ray and NMR structures are superimposed, the rms differences between CA atoms average 3.4 Å for NMR structure 4, 3.0 Å for 12, 6.8 Å for 8, and 7.5 Å for 9. When the dimers are superimposed, the rms differences between the CA atoms increase to 5.2 Å for 4, 5.8 Å for 12, 9.7 Å for 8, and 8.1 Å for 9. The deviations of the NMR structures from the crystal structure generally involve the position of loop I in relation to the rest of each subunit, but they also involve some minor differences of the other loops as well.

The dimer interface in the NMR structures was described as being stabilized by direct hydrophobic interactions between the aromatic rings of Phe 49 and Phe 49′ and the side chains of Leu 57 and Leu 57′. The current crystal structure confirms the basic chain orientation and the general location of the dimer interface, as described in the NMR study, but indicates the lack of any direct interaction between Phe 49 and Phe 49′ whose ring centroids are 12.8 Å apart. The side chains of Leu 57 and Leu 57′ do, however, interact as the NMR study suggested. In addition, the NMR structure also shows four hydrogen bonds across the dimer interface, while the crystal structure suggests that there are nine such interactions.

The hydrogen-bonding interactions noted above between Ile 20 and Val 43 were not observed in the NMR study (Oswald et al., 1991), as the exchange rate of the amide proton of Ile 20 was found to be rapid. The amide proton exchange rate for Ser 55 was slow, however, suggesting a hydrogen bond with the carbonyl of Ala 25. The crystal structure indicates that these two hydrogen bonds are rather long, which would be consistent with the tentative nature of these interactions assigned from the NMR work.

Comparison with Related α-Neurotoxin X-ray Structures. The amino acid sequences of 84 α-neurotoxins and 4 κ-neurotoxins have been reported (Endo & Tamiya, 1991), as have the X-ray structures of the snake venom α-neurotoxins noted above. The α-neurotoxins are classified as either short (60–62 residues, four disulfide bridges) or long (70–74 residues, five disulfide bridges). κ-Bungarotoxin contains features that are intermediate between those of the short and long α-neurotoxins. For example, κ-bungarotoxin contains five disulfide bridges like the long α-neurotoxins, a short C-terminal tail like the short α-neurotoxins, and an intermediate number of 66 amino acid residues (Fiordalisi et al., 1994a).

A comparison of the structures of κ-bungarotoxin, α-bungarotoxin, α-cobratoxin, and erabutoxins *a* and *b* indicates that the overall polypeptide fold of the subunits is similar. In agreement with the NMR structure (Oswald et al., 1991; Sutcliffe et al., 1992), the X-ray structure shows no consistent differences in the nature of the electrostatic surface of κ-bungarotoxin when compared to the four α-neurotoxins. The most significant surface charge difference seen in κ-bungarotoxin occurs at the tip of loop II, where a Lys residue is found at position 29. However, a positively charged residue is found here in only two of the four κ-neurotoxins sequenced: Lys in κ-bungarotoxin and Arg in κ-flavitoxin. κ_2- and κ_3-bungarotoxin contain a Gln and an Asn residue at this position, respectively (Fiordalisi et al., 1994a). This suggests that if an additional positive charge is important for specificity, the other two κ-neurotoxins must contain compensating positively charged residues located in the same general vicinity, possibly Arg 50 at the tip of loop III.

The position of the invariant Trp residue present in all active α-neurotoxins, but not in any of the κ-neurotoxins, is clearly seen on the surface of the α-neurotoxin structures. κ-Bungarotoxin contains Gln 26 at this position and its interactions have been noted (Table 5). It is unlikely, however, that this difference plays a significant role in neurotoxin specificity, since mutagenesis studies with κ-bungarotoxin (Fiordalisi et al., 1994a) indicate that the replacement of Gln 26 with a Trp residue has no effect on the ability of κ-bungarotoxin to inhibit nerve transmission in chick ciliary ganglia. However, this mutation appears to increase the affinity of κ-bungarotoxin for the neuromuscular receptor by an order of magnitude (Fiordalisi et al., 1994b). Conversely, Pillet et al. (1993) demonstrated that mutating this Trp to Phe or His reduced the affinity of erabutoxin *a* for the neuromuscular receptor by 1–2 orders of magnitude. Thus, a Trp residue at this position appears to be more important for interaction with the neuromuscular receptor than for the κ-bungarotoxin-sensitive neuronal receptor.

Receptor Binding of α- and κ-Neurotoxins. Mutagenesis studies of α- and κ-neurotoxins (Pillet et al., 1993; Fiordalisi et al., 1994a), as well as a large number of chemical modification studies [reviewed in Endo and Tamiya (1991)], have shown that Arg 34, a conserved residue in all active postsynaptic neurotoxins, is the most critical residue for receptor binding and inhibition of nerve transmission of all residues studied.

This residue is located near the tip of loop II between strands C and D in all neurotoxins. Mutagenesis studies on flanking residues in κ-bungarotoxin (Fiordalisi et al., 1994a) have failed, however, to discern the basis for toxin–receptor specificity. For example, studies with κ-bungarotoxin have indicated that the most conserved residues in this loop, specifically Pro 36, which is found in all κ-neurotoxins and no α-neurotoxins, and the Trp residue, which is found in all α-neurotoxins but no κ-neurotoxins, exert little effect on nerve transmission in chick ciliary ganglia. Therefore, while Arg 34 appears to be essential in all neurotoxins, the basis for the differential selectivity of α- and κ-neurotoxins remains unclear on the basis of the available mutagenesis and chemical modification data.

The tips of loops II and II′, containing the crucial Arg 34 side chains, are pointing in opposite directions in the κ-bungarotoxin dimer (Figures 1 and 2). If the dimer is the key to κ-bungarotoxin specificity, it may function to link the two receptor binding regions of the toxin together so that they bind in concert, perhaps one to each α-subunit of the receptor. The distance between acetylcholine binding sites on the two α-subunits of the nicotinic acetylcholine receptor pentamer from the electric organ of *Torpedo californica* has been determined to be 30–50 Å (Herz et al., 1989), and the distance between α-bungarotoxin binding sites on the *Torpedo marmorata* receptor is 42 Å (Unwin, 1993). The distance between the guanidinium groups of Arg 34 and Arg 34′ of the κ-bungarotoxin dimer is ~44 Å (Arg 34—CZ···Arg 34′—CZ = 43.8 Å). Thus, the experimentally determined dimensions are consistent with the idea that a κ-bungarotoxin dimer may interact in concert with both α-subunits in a receptor. The putative cross-link between α-subunits thus formed may function to inhibit the opening of the ion channel of the receptor. This interpretation would suggest that the mode of binding and inhibition of κ-bungarotoxin for its receptor may be different from that of α-bungarotoxin for its receptor. In other words, this explanation could not apply to the neuromuscular receptors, which are inhibited selectively by the monomeric α-neurotoxins. Similarly, there would have to be some reason why one end of a κ-bungarotoxin dimer does not interact effectively with the neuromuscular receptor site. This concept is consistent with observations that the α-neurotoxins may bind to different areas of their respective α-subunits than do the κ-neurotoxins. It should be noted that this hypothesis is compatible with a recent NMR study (Basus et al., 1993) of a complex of α-bungarotoxin and a peptide derived from the nicotinic receptor. In this structure, the peptide binds to the three-stranded β-sheet of the α-toxin to form a four-stranded β-sheet.

Several studies have confirmed that specific peptides isolated from, or based on, the *Torpedo* acetylcholine receptor α-subunit bind to α-bungarotoxin (Lentz & Wilson, 1988; McLane et al., 1993). This was confirmed using synthetic peptides for the *Torpedo* receptor vertebrate muscle α1-subunit and avian brain α7- and α8-subunits (Conti-Tronconi et al., 1990; McLane et al., 1991a,b). The region identified in these studies differs from the principal sequence for κ-neurotoxin binding on α3-subunits, although the primary α3-subunit sequence is homologous to a secondary sequence for α-bungarotoxin from the α1-subunit (McLane et al., 1990a,b).

The high-resolution X-ray structure of κ-bungarotoxin now provides a firm basis upon which to plan further investigations into the basis of the physiological specificity between the α- and κ-neurotoxins and their interactions with their respective receptors.

ACKNOWLEDGMENT

We thank J. Fiordalisi, A. Kromminga, S. Patel, and G. Scapin for their assistance with various aspects of this work.

REFERENCES

Basus, V. J., Billeter, M., Love, R. A., Stroud, R. M., & Kuntz, I. D. (1988) *Biochemistry 27*, 2763–2771.
Basus, V. J., Song, G., & Hawrot, E. (1993) *Biochemistry 32*, 12290–12298.
Bernstein, F. C., Koetzle, T. F., Williams, G. J. B., Meyer, E. F., Brice, M. D., Rodgers, J. R., Kennard, O., Shimanouchi, T., & Tasumi, M. (1977) *J. Mol. Biol. 112*, 535–542.
Betzel, C., Lange, G., Pal, G. P., Wilson, K. S., Maelicke, A., & Saenger, W. (1991) *J. Biol. Chem. 266*, 21530–21536.
Blundell, T. L., & Johnson, L. N. (1976) *Protein Crystallography*, Academic Press, London.
Bourne, P. E., Sato, A., Corfield, P. W. R., Rosen, L. S., Birken, S., & Low, B. W. (1985) *Eur. J. Biochem. 153*, 521–527.
Brünger, A. T. (1992) *X-PLOR. A System for X-ray Crystallography and NMR*, Version 3.1, Yale University Press, New Haven, CT.
Brünger, A. T., Krukowski, A., & Erickson, J. W. (1990) *Acta Crystallogr. A46*, 585–593.
Burley, S. K., & Petsko, G. A. (1985) *Science 229*, 23–28.
Chiappinelli, V. A. (1983) *Brain Res. 227*, 9–22.
Chiappinelli, V. A., & Zigmond, R. E. (1978) *Proc. Natl. Acad. Sci. U.S.A. 75*, 2999–3003.
Chiappinelli, V. A., & Dryer, S. E. (1984) *Neurosci. Lett. 50*, 239–244.
Chiappinelli, V. A., & Lee, J. C. (1985) *J. Biol. Chem. 260*, 6182–6186.
Conti-Tronconi, B. M., Tang, F., Diethelm, B. M., Spencer, S. R., Reinhardt-Maelicke, S., & Maelicke, A. (1990) *Biochemistry 29*, 6221–6230.
Corfield, P. W. R., Lee, T.-J., & Low, B. W. (1989) *J. Biol. Chem. 264*, 9239–9242.
Endo, T., & Tamiya, N. (1991) in *Snake Toxins* (Harvey, A. L., Ed.) pp 165–222, Pergamon Press, New York.
Engh, R. A., & Huber, R. (1991) *Acta Crystallogr. A47*, 392–400.
Fiordalisi, J. J. (1994) Ph.D. Thesis, Washington University School of Medicine, St. Louis, MO.
Fiordalisi, J. J., & Grant G. A. (1994) in *Techniques in Protein Chemistry V* (Crabb, J., Ed.) pp 269–274, Academic Press, San Diego.
Fiordalisi, J. J., Al-Rabiee, R., Chiappinelli, V. A., & Grant, G. A. (1994a) *Biochemistry 33*, 3872–3877.
Fiordalisi, J. J., Al-Rabiee, R., Chiappinelli, V. A., & Grant, G. A. (1994b) *Biochemistry* (in press).
Furey, W., & Swaminathan, S. (1990) *Proc. Am. Crystallogr. Assoc. Meet. (New Orleans)*, Abstract PA33.
Galzi, J.-L., Revah, F., Bessis, A., & Changeux, J.-P. (1991) *Annu. Rev. Pharmacol. 31*, 37–72.
Grant, G. A., & Chiappinelli, V. A. (1985) *Biochemistry 24*, 1532–1537.
Herz, J. M., Johnson, D. A., & Taylor, P. (1989) *J. Biol. Chem. 264*, 12439–12448.
Hider, R. C., Drake, A. F., Inagaki, F., Williams, R. J. P., Endo, T., & Miyazawa, T. (1982) *J. Mol. Biol. 158*, 275–291.
Inagaki, F., Hider, R. C., Hodges, S. J., & Drake, A. F. (1985) *J. Mol. Biol. 183*, 575–590.
Jones, T. A. (1985) *Methods Enzymol. 115*, 157–171.
Kraulis, P. J. (1991) *J. Appl. Crystallogr. 24*, 946–950.
Labhardt, A. M., Hunziker-Kwik, E. H., & Wüthrich, K. (1988) *Eur. J. Biochem. 177*, 295–305.
Laskowski, R. A., MacArthur, M. W., Moss, D. S., & Thornton, J. M. (1993) *J. Appl. Crystallogr. 26*, 283–291.
le Du, M. H., Marchot, P., Bougis, P. E., & Fontecilla-Camps, J. C. (1992) *J. Biol. Chem. 267*, 22122–22130.
Lentz, T. L., & Wilson, P. T. (1988) *Int. Rev. Neurobiol. 29*, 117–160.

Love, R. A., & Stroud, R. M. (1986) *Protein Eng. 1*, 37–46.
Low, B. W. (1979) in *Handbook of Experimental Pharmacology* (Lee, C. Y., Ed.) Vol. 52, pp 213–257, Springer-Verlag, Berlin.
Low, B. W., & Corfield, P. W. R. (1986) *Eur. J. Biochem. 161*, 579–587.
Low, B. W., & Corfield, P. W. R. (1987) *Asia Pac. J. Pharmacol. 2*, 115–127.
Low, B. W., Preston, H. S., Sato, A., Rosen, L. S., Searl, J. E., Rudko, A. D., & Richardson, J. S. (1976) *Proc. Natl. Acad. Sci. U.S.A. 73*, 2991–2994.
McLane, K. E., Tang, F., & Conti-Tronconi, B. M. (1990a) *J. Biol. Chem. 265*, 1537–1544.
McLane, K. E., Wu, X., & Conti-Tronconi, B. M. (1990b) *J. Biol. Chem. 265*, 9816–9824.
McLane, K. E., Wu, X., Diethelm, B., & Conti-Tronconi, B. M. (1991a) *Biochemistry 30*, 4925–4934.
McLane, K. E., Wu, X., & Conti-Tronconi, B. M. (1991b) *Biochemistry 30*, 10730–10738.
McLane, K. E., Dunn, S. M., Conti-Tronconi, B. M., & Rafferty, M. A. (1993) in *Handbook of Protein and Peptide Design* (Carey, P., Ed.) Academic Press, New York.
Oswald, R. E., Sutcliffe, M. J., Bamberger, M., Loring, R. H., Braswell, E., & Dobson, C. M. (1991) *Biochemistry 30*, 4901–4909.
Pillet, L., Trémeau, O., Ducancel, F., Drevet, P., Zinn-Justin, S., Pinkasfeld, S., Boulain, J.-C., & Ménez, A. (1993) *J. Biol. Chem. 268*, 909–916.
Priestle, J. P. (1993) in *Joint CCP4 and ESF-EACBM Newsletter on Protein Crystallography* (Bailey, S., & Wilson, K. S., Eds.) November issue, No. 29, Daresbury Laboratory, Warrington, UK.
Rees, B., & Bilwes, A. (1993) *Chem. Res. Toxicol. 6*, 385–406.
Rees, B., Bilwes, A., Samama, J. P., & Moras, D. (1990) *J. Mol. Biol. 214*, 281–297.
Richardson, J. S. (1981) *Adv. Protein Chem. 34*, 167–339.
Rodriguez-Ithurralde, D., Silveira, L., Barbeito, L., & Dajas, F. (1983) *Neurochem. Int. 5*, 267–274.
Sacchettini, J. C., Patel, S., Scapin, G., Fiordalisi, J. J., & Grant, G. A. (1992) *J. Mol. Biol. 226*, 559–562.
Salemme, F. R., & Weatherford, D. W. (1981) *J. Mol. Biol. 146*, 101–117.
Smith, J. L., Corfield, P. W. R., Hendrickson, W. A., & Low, B. W. (1988) *Acta Crystallogr. A44*, 357–368.
Sutcliffe, M. J., Dobson, C. M., & Oswald, R. E. (1992) *Biochemistry 31*, 2962–2970.
Tronrud, D. E., Ten Eyck, L. F., & Matthews, B. W. (1988) *Acta Crystallogr. A43*, 489–501.
Tsernoglou, D., & Petsko, G. A. (1976) *FEBS Lett. 68*, 1–4.
Unwin, N. (1993) *J. Mol. Biol. 229*, 1101–1124.
Wang, B. C. (1985) *Methods Enzymol. 115*, 90–112.